

# Biomimetic 3D Clusters Using Human Adipose Derived Mesenchymal Stem Cells and Breast Cancer Cells: A Study on Migration and Invasion of Breast Cancer Cells

Min Hee Park,<sup>†</sup> Boa Song,<sup>†,‡</sup> Seungpyo Hong,<sup>‡,#</sup> Sang Heon Kim,<sup>\*,†,‡</sup> and Kangwon Lee<sup>\*,§,||</sup>

<sup>†</sup>Center for Biomaterials, Korea Institute of Science and Technology, Seoul 02792, Republic of Korea

<sup>‡</sup>Department of Biomedical Engineering, University of Science and Technology, Daejeon 34113, Republic of Korea

<sup>‡</sup>Department of Biopharmaceutical Sciences, University of Illinois, Chicago, Illinois 60612, United States

<sup>#</sup>Department of Integrated OMICS for Biomedical Science and Underwood International College, Yonsei University, Seoul 03706, Republic of Korea

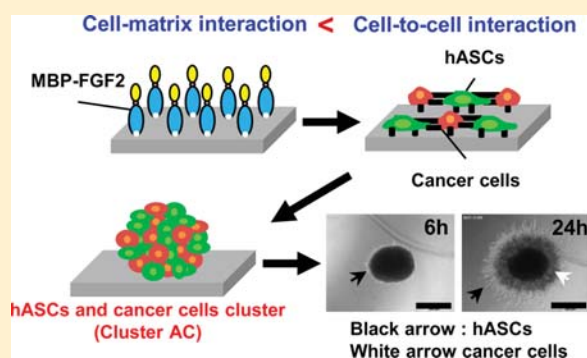
<sup>§</sup>Program in Nanoscience and Technology, Graduate School of Convergence Science and Technology, Seoul National University, Seoul 08826, Republic of Korea

<sup>||</sup>Advanced Institutes of Convergence Technology, Gyeonggi-do 16229, Republic of Korea

## Supporting Information

**ABSTRACT:** Invasion and metastasis of cancer directly related to human death have been associated with interactions among many different types of cells and three-dimensional (3D) tissue matrices. Precise mechanisms related to cancer invasion and metastasis still remain unknown due to their complexities. Development of tumor microenvironment (TME)-mimicking system could play a key role in understanding cancer environments and in elucidating the relating phenomena and their driving forces. Here we report a facile and novel platform of 3D cancer cell-clusters using human adipose-derived mesenchymal stem cells (hASCs) and breast cancer cells (MDA-MB-231) within a collagen gel matrix to show cancer invasion in the cell and extracellular matrix (ECM). Both clusters A (hASC only) and AC (hASC and MDA-MB-231) exhibited different behaviors and expressions of migration and invasion, as observed by the relating markers such as fibronectin,  $\alpha$ -SMA, and CXCR4. hASCs showed a protrusive migration from a cluster center, whereas MDA-MB-231 spread out radially followed by hASC migration. Finally, the effect of matrix was further discussed by varying collagen gel densities. The new biomimetic system of 3D cancer clusters developed here has the potential to be utilized for research on migration and invasion of cancer cells in extracellular matrices.

**KEYWORDS:** cell cluster, collagen gel, migration, invasion, tumor microenvironment



invasion and metastasis.<sup>1,2</sup> Invasive and metastatic tumors are known to be heterogeneous as they contain a variety of subpopulations of cells with different metastatic potentials.<sup>3</sup> Cellular heterogeneity in cancer tissues has been reported in epithelial cells. Moreover, a study on mammalian carcinoma showed greater differentiation of neoplastic stem cells compared to that in analogous noncancer tissues resulting in tumor heterogeneity.<sup>4</sup> In addition, another study reported that

## INTRODUCTION

Invasion and metastasis are responsible for approximately 90% of deaths caused by cancer. Metastasis is a highly complicated phenomenon that is associated with many different types of cells, connective tissues, and blood vessel components within different organs. Better understanding of cancer invasion and metastasis is key to the development of effective cancer intervention methods including anticancer drugs. Well-defined tissue models, instead of more complicated in vivo models, would be ideal to perform systematic studies, particularly during the early development stages. However, most cancer models that are currently available fail to faithfully mimic cancer environments.

Several studies have focused on better mimicking cancer environments and understanding the processes of cancer

invasion and metastasis.<sup>1,2</sup> Invasive and metastatic tumors are known to be heterogeneous as they contain a variety of subpopulations of cells with different metastatic potentials.<sup>3</sup> Cellular heterogeneity in cancer tissues has been reported in epithelial cells. Moreover, a study on mammalian carcinoma showed greater differentiation of neoplastic stem cells compared to that in analogous noncancer tissues resulting in tumor heterogeneity.<sup>4</sup> In addition, another study reported that

**Special Issue:** Physics-Inspired Micro/Nanotherapeutics

**Received:** December 17, 2015

**Revised:** May 4, 2016

**Accepted:** May 10, 2016

**Published:** May 10, 2016

stem cell biology could provide new insight into cancer biology. This study also proposes that tumors may contain a considerable amount of cancer stem cells.<sup>5</sup> This is direct evidence that the behavior and fate of cancer cells rely on the tumor microenvironment (TME). Martin et al. also showed that mesenchymal stem cells (MSCs) have an influence on cell growth and metastasis through the regulation of epithelial-to-mesenchymal transition (EMT)-associated genes.<sup>6</sup>

Construction of TME is the first step in studying cancer invasion and metastasis and the related tumor initiation, progression, and responses to therapy. There have been numerous studies showing that 3D cancer cell aggregates or cancer clusters offer a similar TME.<sup>7–9</sup> A natural biological system including a solid tumor in a human body, is a three-dimensional (3D) environment, providing a 3D matrix for cancer cells.<sup>10,11</sup> Compared to traditional cell cultures on a 2D system, the cells and tissues in 3D microenvironments undergo dramatic changes in cell phenotypes and biomarker expressions. Furthermore, genetic and external environmental factors, along with the physical and mechanical factors applied to cancer cells, are known to affect the invasion and metastasis behaviors of the cells in tissues and organs. For example, stiffer matrices formed by collagen deposition can enhance cell proliferation and invasion. In addition, circulating tumor cells (CTCs) are significantly affected by shear flow during intravasation and extravasation.<sup>12,13</sup>

It has been reported that 3D cell aggregates were formed by controlling the strength balance between cell-matrix adhesion and cell-to-cell contact.<sup>14</sup> A number of researchers showed that fibronectin plays a major role in cellular morphology and function through cell-fibronectin interactions.<sup>15</sup> Attachment to the RGD motif of fibronectin is mediated primarily by the  $\beta 1$  subunit of integrin. Integrins are a family of cell adhesion receptors linking the ECM to intracellular signaling molecules and the cytoskeleton network. In addition to the RGD motif, other domains of fibronectin can promote the attachment of specific cells.<sup>16,17</sup> Previously, we reported that heparan sulfate proteoglycans (HSPGs) on the membrane of hASCs are involved in cell adhesion through interactions with the heparin-binding domain of fibronectin. The basic fibroblast growth factors (FGF2) are molecules having affinity to HSPG.<sup>18,19</sup> A simple method to immobilize FGF2 to hydrophobic surfaces was introduced using maltose binding protein (MBP) as a physical linker, which was designed to induce HSPG-mediated stem cell adhesion.<sup>20</sup> We demonstrated that hASCs adhered to a surface coated with MBP-FGF2 through HSPG-mediated interaction and integrin-mediated adhesion were restricted in hASCs adhered to the surface to cause a reduction in cell-matrix adhesive force.<sup>21</sup> A hydrophobic polystyrene surface coated with MBP-FGF2 was used to generate a spheroid type 3D cluster of hASCs, resulting in weakening cell-matrix adhesion of 3D cell mass (3DCM). Recently, we have developed the 3DCM of hASCs as an injectable microtissue in cell-based regenerative medicine.<sup>22</sup>

In this article, we report a facile and novel platform of 3D cancer cell-clusters consisting of either hASCs only (cluster A) or a mixture of hASCs and breast cancer cells (MDA-MB-231) (cluster AC) within a collagen gel matrix to show cancer cell invasion in cell and matrix environments. The morphological changes and migration behaviors of the clusters were monitored over time when the clusters were prepared in various concentrations of collagen gels. We investigated the expression levels of migration and invasion markers, such as

CD44, fibronectin,  $\alpha$ -SMA, and CXCR4, in the clusters. Furthermore, we found that the biophysical regulation of the breast cancer cells was affected by the cocultured system and matrices that is biomimetic to TME. This novel biomimetic system of 3D cancer/stem cell clusters has potential to offer a reliable model for research on migration and invasion of cancer cells.

## ■ EXPERIMENTAL SECTION

**Materials.** hASCs and MDA-MB-231 were obtained from Cefobio (Seoul, Korea) and American Type Culture Collection (Manassas, VA, USA), respectively. Rat tail collagen I used in this study was purchased from Corning (Corning, NY, USA). The Live–Dead Cell Staining Kit was purchased from BioVision (Seoul, Korea), and all antibodies used for immunofluorescence assays were obtained from Abcam (Cambridge, U.K.).

**Cell Culture.** hASCs (passage 6) were cultured under 5% CO<sub>2</sub> atmosphere at 37 °C by using an hASC growth medium (Cefobio, Korea) containing supplement and 1% penicillin/streptomycin. The medium was replaced every 3 days. MDA-MB-231 was maintained in RPMI 1640 medium supplemented with 10% fetal bovine serum (FBS) and 1% penicillin/streptomycin. The medium was replaced every 2 days.

**Preparation of the MBP-FGF2 Surface.** The MBP-FGF2 surfaces were prepared using our previously published protocol.<sup>21,23</sup> Briefly, MBP-FGF2 fusion protein was obtained from *Escherichia coli* carrying pMAL-FGF2 plasmids that were generated by the insertion of human FGF2 complement DNA (cDNA) (Bioneer, Korea) into the pMAL vector (New England Biolabs, U.K.). Human FGF2 165 cDNA was cloned from human fibroblasts by means of polymerase chain reaction (PCR) using oligonucleotide pairs (Bioneer; 5'-CCGAA-TTCCCCGCCTTGCCCGAGGATGGC-3' and 5'-CAAAG-CTTTTCAGCTCTTAGCAGACATTGGAAG-3') including *EcoR I* and *Hind III* restriction sites, respectively. The PCR products were cloned into plasmid pGEM-T (Promega, USA) to generate pGEM-FGF2. The pGEM-FGF2 and plasmid pMAL were digested using *EcoR I*-*Hind III* and recovered from an agarose gel. The digested fragments were ligated using a ligation kit (Takara, Japan) to generate pMAL-FGF2. MBP-FGF2 (20  $\mu$ g/mL) was spontaneously adsorbed to a polystyrene (PS) surface plates (nontissue culture-treated plate, 96- or 384-well plates; Falcon, Fisher Scientific, USA) at 37 °C for 4 h.<sup>21,22,24</sup>

**Preparation of Clusters A and AC.** hASCs or hASCs/MDA-MB-231 suspensions were seeded on a MBP-FGF2-coated 96- or 384-well PS plate in the hASC growth medium (Cefobio, Korea). The medium was supplemented and cultured for 1 day in an incubator at 37 °C. After 24 h of culture, clusters A and AC were observed using an Axio Vert.A1 inverted microscope (Zeiss, Germany).

**Viability and Morphology.** For the live–dead cell assay, after 24 h, clusters A and AC were stained using the Live–Dead Cell Staining Kit (BioVision, Korea) for 1 h according to the manufacturer's protocol. After washing with PBS, the clusters were fixed in a formaldehyde solution and embedded into the optimal cutting temperature (O.C.T.) compound (SAKURA Tissue-Tek, USA) for 12 h and then frozen. The frozen clusters were sectioned into 10  $\mu$ m thick samples at –20 °C and attached to glass slides. Clusters A and AC were encapsulated in collagen gels prepared using Rat tail collagen I at concentrations of 2, 4, and 6 mg/mL and fixed in a

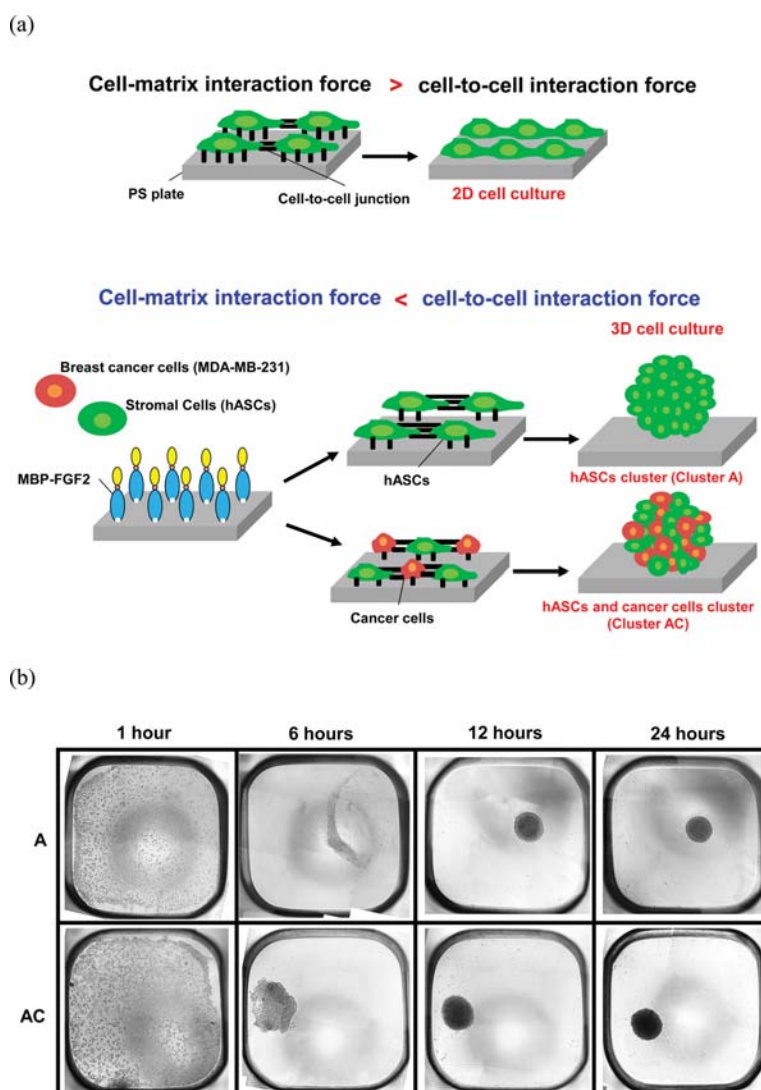


**Figure 1.** (a) Scheme for the formation of clusters A and AC through control of cell-matrix or cell-to-cell interaction on a substrate with immobilized MBP-FGF2. (b) Behavior of hASCs and MDA-MB-231 on MBP-FGF2 coated PS-plate during cluster formation. Cell density of hASCs and MDA-MB-231 were 10000 cells per well in a 384-well PS-plate, respectively. After 1 h, we observed the rolled up cell sheet, and then formed the cell cluster at 12 h. The scale bar is 200  $\mu\text{m}$ .

formaldehyde solution. The fixed gels were then embedded into the O.C.T. compound for 12 h and frozen. The frozen gel samples were sectioned into 10  $\mu\text{m}$  thick sections at  $-20\text{ }^{\circ}\text{C}$  and attached to the glass slides. The behaviors of clusters A and AC within the collagen gels were monitored using the Axio Observer microscope (Zeiss, Germany) over incubation of 0, 6, 12, 24, and 48 h. Prior to cluster formation, PKH67 labeled hASCs (PKH67 Green Fluorescent Cell Linker Mini Kit, Sigma, USA) and PKH26 labeled MDA-MB-231 (PKH26 Red Fluorescent Cell Linker Mini Kit, Sigma, USA) were seeded on a MBP-FGF2-coated 384-well PS plate in the hASC growth medium (Cefobio, Korea). At each of the concentrations of collagen gels and the incubation hours, cell migration was defined by the distance the cells traveled from the center of the clusters measured using ImageJ software.

**Scanning Electron Microscopy.** The scanning electron microscope (SEM) images of clusters A and AC were obtained after formation of the clusters. After washing with PBS, the clusters were fixed in 2.5% glutaraldehyde solution at  $4\text{ }^{\circ}\text{C}$  for

30 min. The fixed clusters were maintained in the 2% osmium tetroxide ( $\text{OSO}_4$ ) for 2 h at  $4\text{ }^{\circ}\text{C}$ , and washed with deionized water. After dehydration with dilute ethanol, the clusters were dried by evaporation using hexamethyldisilazane (HMDS) and stored in a vacuum chamber for 1 day before the imaging experiments. SEM images were then acquired using FE-SEM Hitachi S 4100 (Hitachi, Japan).

**Immunofluorescence Staining.** For the immunofluorescence study to measure expression levels of CD44, fibronectin,  $\alpha$ -SMA, and CXCR4, sections of clusters A- and AC-injected collagen gels were incubated at  $4\text{ }^{\circ}\text{C}$  with the corresponding primary antibodies (Abcam, U.K.). After washing the sections with PBS, antibody staining was performed using secondary antibodies (Abcam, U.K.) according to the manufacturer's protocol. Then, the sections were incubated with 4',6'-diamidino-2-phenyl indole (DAPI) (Thermo Fisher Scientific, USA) for nucleus staining followed by actin staining using rhodamine phalloidin (Thermo Fisher Scientific, USA). The fluorescently labeled cells were finally

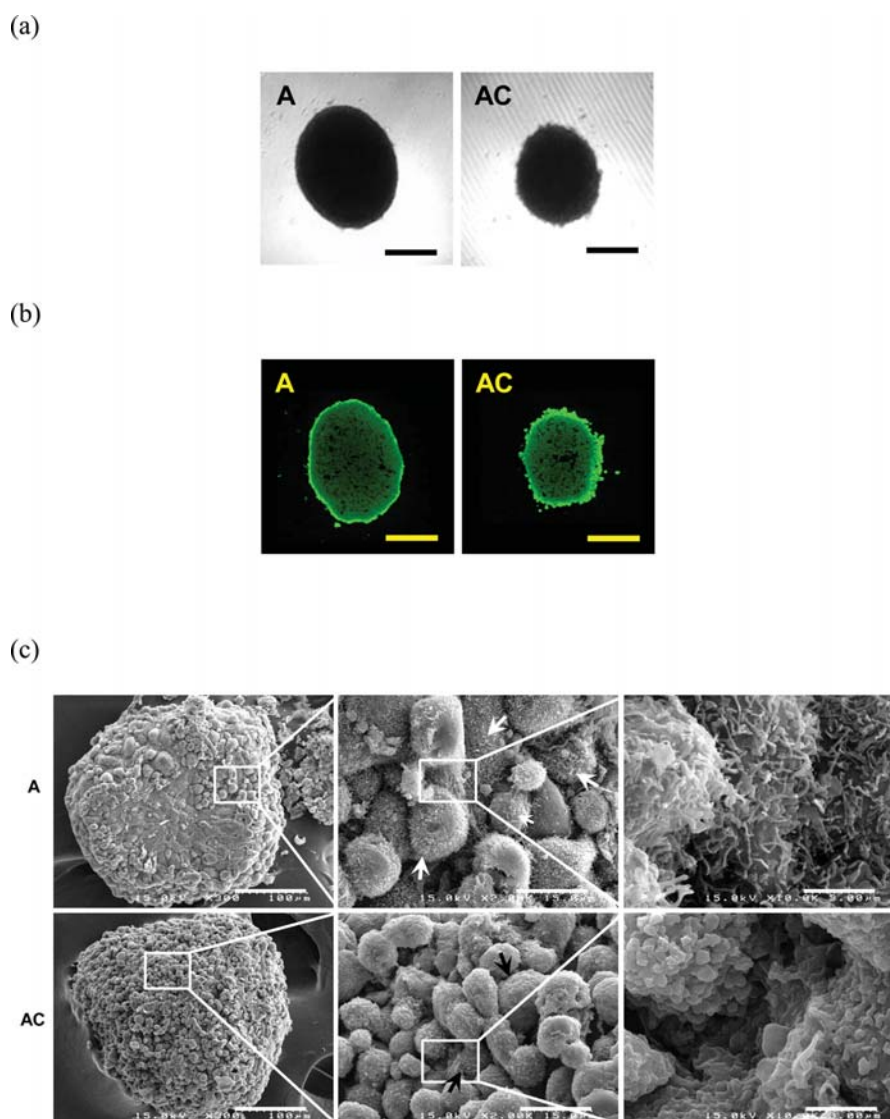


**Figure 2.** (a) Morphology and (b) viability of cluster A and AC on MBP-FGF2 coated PS-plate at 24 h. The scale bar is 200  $\mu\text{m}$ . (c) SEM image of cluster A and AC. The white and black arrow indicates ECM fiber and hASC. hASCs shows bigger than breast cancer cells. The scale bar is 100, 15, and 3  $\mu\text{m}$ , respectively.

observed under a LSM 700 laser scanning confocal microscope (Zeiss, Germany).

**Statistical Analysis.** Quantitative data were expressed as mean  $\pm$  standard error of the mean (SE). The significance of differences in the mean values was evaluated using the one-way ANOVA with Tukey tests. Differences were considered significant when the  $p$  value was less than 0.05 (marked as \*).

## RESULTS AND DISCUSSION

**Formation of Clusters A and AC.** We examined whether a cocluster composed of hASCs and MDA-MB-231 was formed on MBP-FGF2-coated PS plates. Figure 1a shows a scheme for formation of clusters A and AC. We obtained clusters A and AC (Figure 1b) by culturing hASCs and the mixture of hASCs and MDA-MB-231 cells in 3D, respectively, on the MBP-FGF2-coated PS plates. The mechanism of the 3D cluster formation of hASCs is biophysically explained by the strength balance between cell-ECM-cell contact and cell-matrix adhesion, as

shown in Figure 1. For cluster AC, suspension of MDA-MB-231 cells and hASCs were cultured on the MBP-FGF2-coated PS plate. There were numerous approaches of forming spheroid clusters, such as culturing cells in nonstick U-bottom wells, in hanging drop, in rotating wall vessels, etc. Some reports have been shown that MDA-MB-231s were aggregated Matrigel or solid-like gel such as methylcellulose (MethoCel), DEX-in-PEG ATPS, and poly-HEMA.<sup>25–29</sup> On the poly-HEMA coated plates, MDA-MB-231 form loose aggregates of cells after 24 h. The cell–cell interactions established by this method are weak, and the aggregates can be easily regressed mechanically by pipetting without additives such as collagen and reconstituted basement membrane. MDA-MB-231 cells did not form clusters because these epithelial cells do not produce ECMs in our systems (Figure S1). In a similar manner, we believe the reason why MDA-MB-231 does not form a stable cell cluster is because an interaction force between the cells is much weaker than that between cell and the surface coated with

MBP-FGF2, the membrane binding motif. Thus, we used our 3D cluster model to permit rapid experimental manipulations, testing of hypotheses, and reducing nonuniformity. This method allows an efficient formation of 3D coculture model of stromal cells and epithelial cells, offering a uniform cluster formation with various sizes, strengths, and cell populations that are distinct from other methods (Figure S2).

After 24 h, the morphology of clusters A and AC were observed in a 384-well PS plate using phase contrast microscopy (Figure 2a). Live–dead cell assays of clusters A and AC using confocal microscopy differentiate live and dead cells, appearing as green and red colors, respectively (Figure 2b). After 24 h, both clusters A and AC showed healthy cells but with different roughness of the edges. Cluster AC had rougher surface morphology than cluster A. Figure 2c shows the SEM images of clusters A and AC, revealing that hASCs in cluster A are associated and interlinked with the ECM fibers (white arrow) surrounding the cell membrane surfaces. In contrast, cluster AC did not show the ECM fibers. This result indicates different cell-ECM-cell interactions in cluster AC from that in cluster A during the cluster formation. Collective cell behaviors are defined as an orchestrated movement among interconnected cell groups.<sup>30</sup> It is exploited by cancer cells as an efficient invasion strategy that can be modeled in the laboratory.<sup>31</sup> The ECM remodeling surrounding the cells, resulting in a topological rearrangement of ECM fibers that in turn shape the tissue microenvironment or promote invasive phenotypes.<sup>32</sup> The formation of ECM fiber might be improved by their biophysical interaction of the cell-ECM-cell contact and cell-matrix adhesion, as illustrated in Figure 1a, which is not the case for cluster AC.

#### Behaviors of Clusters A and AC within Collagen Gels.

In the body, stiffness of a 3D matrix is an important factor for the growth and differentiation of cells.<sup>2,33</sup> In addition, microenvironments can regulate cell function and tissue integrity, including migration and alterations in cell-to-cell and cell-matrix adhesions. The elasticity and stiffness of tissues have been reported to be linked to cancer biology.<sup>34,35</sup> For example, cancer progression in soft tissues is correlated with an increase in stiffness due to local accumulation, often caused by cross-linked collagen matrices of the tumor via physical interactions.

We prepared clusters A and AC within collagen gels with different matrix densities.<sup>36</sup> To study different matrices that mimic *in vivo* systems, collagen concentrations of 2, 4, and 6 mg/mL were used for this study. The storage modulus ( $G'$ ) of collagen gel at 25 °C prepared from the collagen solutions carried over 300–500, 800–1800, and 2300–4700 Pa at concentration of 2, 4, and 6 mg/mL, respectively (Figure S3).

The morphological changes of clusters A and AC within the collagen gels were monitored using live cell microscopy (Figure 3a and Video S1). A time-lapse video shows different movement patterns of cell migration from clusters A and AC. Additionally, the fluorescence images of the cells after staining with green and red dyes for hASCs and MDA-MB-231, respectively, indicate that both cells do migrate (Figure 3b). During cell migration, hASCs (black arrow) showed the fibroblast-like escaping behavior from cluster A. However, behaviors of MDA-MB-231 (white arrow) appeared to be drastically different from those of hASCs. Cell migration was measured at 20 spots, as defined by distances from the center of the clusters after 48 h (Figure 3c). This data shows that the concentration of the collagen gels, although modest, affects cell

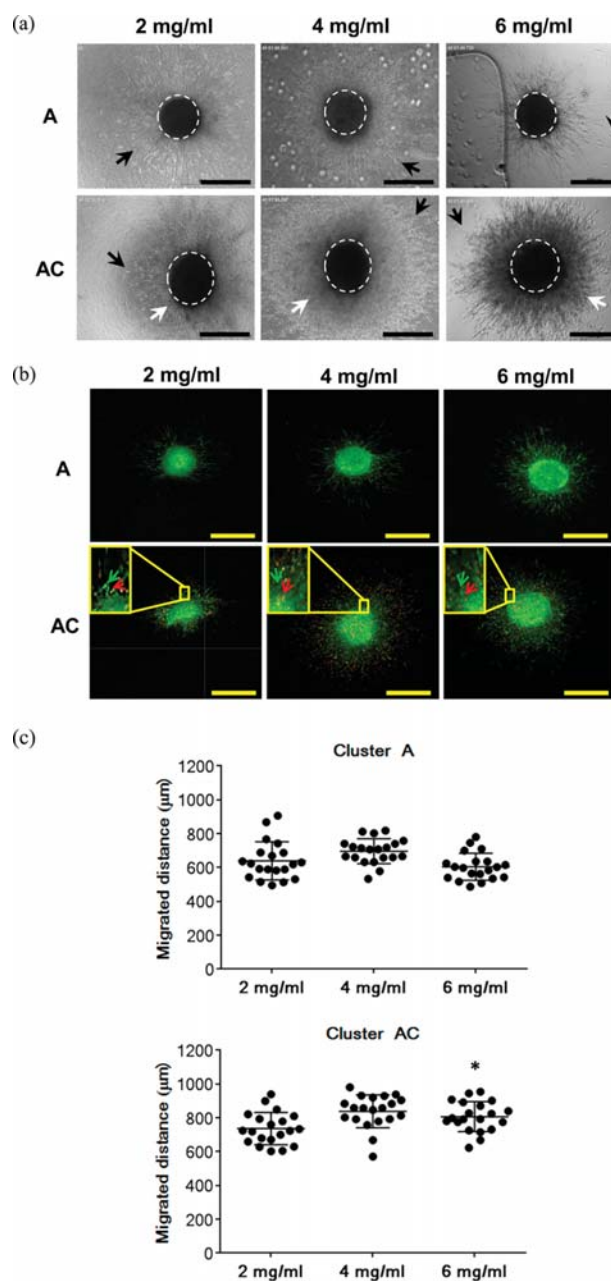


**Figure 3.** (a) Morphological change of clusters A and AC in collagen gel as a function of concentration (2, 4, and 6 mg/mL) at 48 h. The dashed line indicates initial cluster shape. The black and white arrow indicates migrated hASCs and cancer cells. (b) Fluorescence images of clusters A and AC in collagen gel (2, 4, and 6 mg/mL) at 48 h. The inset shows a higher magnified view. The hASCs (green arrow) and MDA-MB-231 (red arrow) stained with PKH67 and PKH27, respectively. The scale bar is 500 μm. (c) Migrated distances (μm) comparison of clusters A and AC in collagen gel (2, 4, and 6 mg/mL) at 48 h. The distance of migrating cells was measured by ImageJ software (mean ± SE,  $n = 20$ ; ANOVA,  $p < 0.05$ ; \* vs 2 mg/mL).

migration. The distance that the cells migrated in a collagen gel of 4 mg/mL (A,  $696.6 \pm 73 \mu\text{m}$ ; AC,  $838.5 \pm 97 \mu\text{m}$ ) was slightly greater compared to that of the cells in a collagen gel concentration of 2 mg/mL (A,  $639.4 \pm 112 \mu\text{m}$ ; AC,  $736.5 \pm 95 \mu\text{m}$ ) or 6 mg/mL (A,  $604.7 \pm 80 \mu\text{m}$ ; AC,  $807.1 \pm 88 \mu\text{m}$ ). Many research groups have investigated responses including

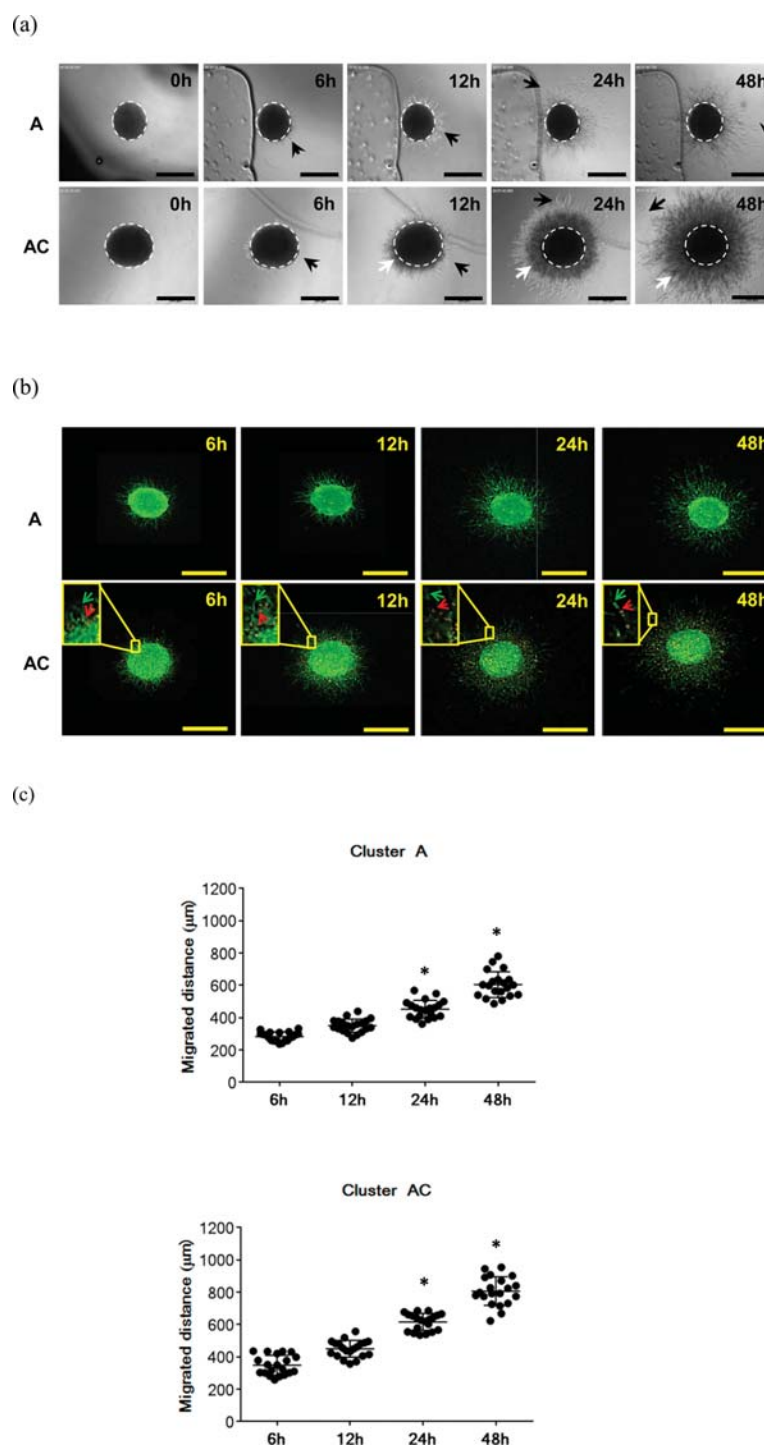


**Figure 4.** (a) Morphological change of clusters A and AC in collagen gel (6 mg/mL) at 0, 6, 12, 24, and 48 h. 0 h indicates time of embedded cluster in collagen gel. The dashed line indicates initial cluster shape. The black and white arrow indicates migrated hASCs and cancer cells. (b) Fluorescence images of cluster A and AC in collagen gel (6 mg/mL). The inset shows a higher magnified view. The hASCs (green arrow) and MDA-MB-231 (red arrow) stained with PKH67 and PKH26, respectively. The scale bar is 500  $\mu\text{m}$ . (c) Migrated distances ( $\mu\text{m}$ ) comparison of clusters A and AC in collagen gel (6 mg/mL) from a time-dependent behavior. The distance of migrating cells was measured by ImageJ software. (mean  $\pm$  SE,  $n = 20$ ; ANOVA,  $p < 0.05$ ; \* vs 0 h).

cell motility in the hydrogels. The cells showed fast movement in stiff hydrogels because the increased stiffness of the gels simultaneously increased the adhesion site density of compounds such as integrin.<sup>37,38</sup> In addition, integrin receptors

and fibronectin appear to play important roles in migration and invasion.<sup>39,40</sup> Thus, we found that the migration behavior of cancer cells escaping from clusters A and AC was governed by collagen gel concentrations.

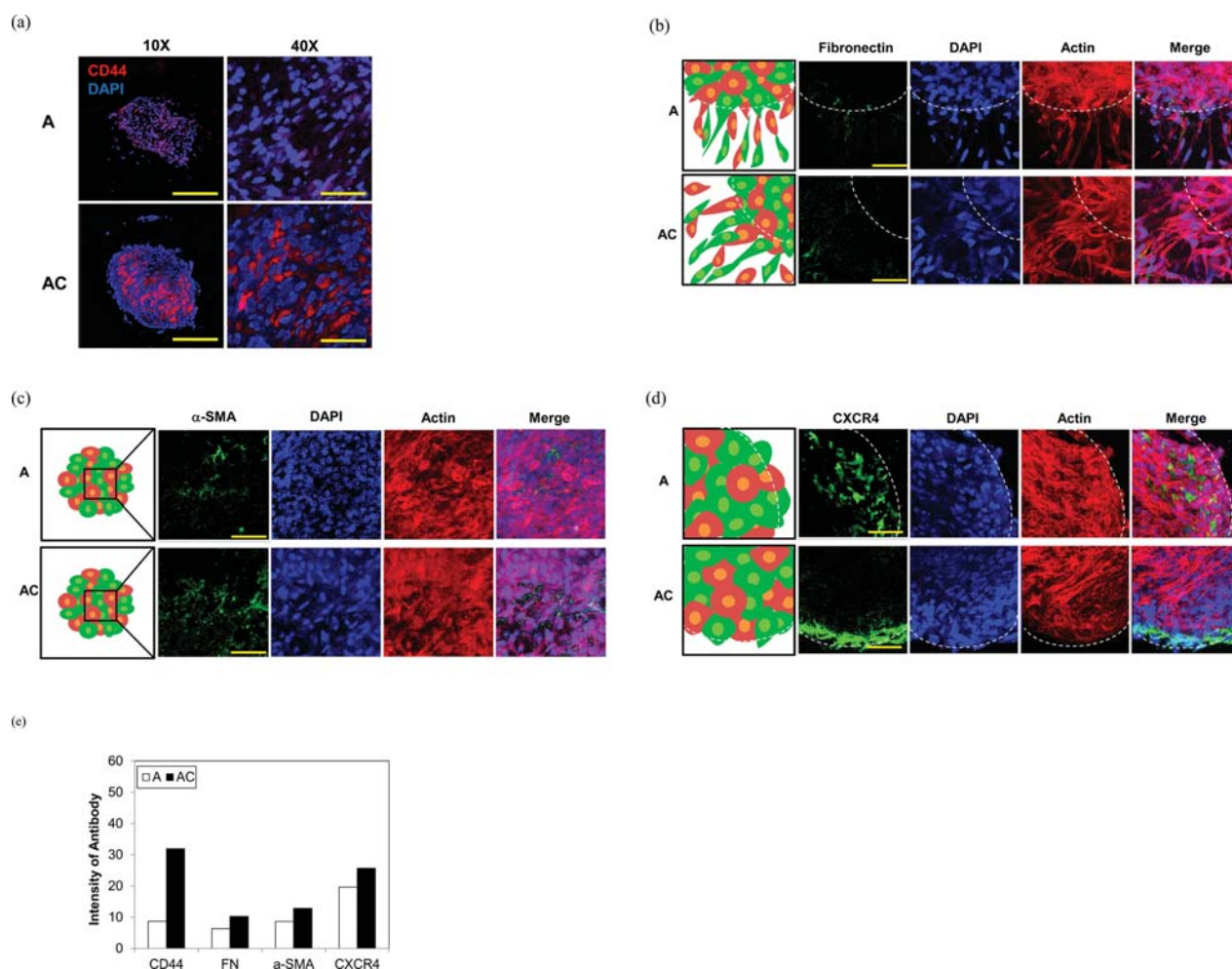


**Figure 5.** Immunofluorescence images of (a) CD44, (b) fibronectin, (c) α-SMA, and (d) CXCR4 expression at clusters A and AC in collagen gel (6 mg/mL) at 48 h. The migration and invasion related marker (green) was stained by Alexa Fluor 488 secondary antibody. The actin (red) and nuclei (blue) of cells are stained by rhodamine phalloidin and 4',6'-diamidino-2-phenyl indole (DAPI). The dashed line indicates cluster boundary. The scale bar is 200 μm (a, low magnification, 10×) and 50 μm (b–d, high magnification, 40×). (e) The intensity of antibodies by ImageJ software.

While normal resident cells in the soft microenvironment of the breast tissues have a shear modulus of around 150 to 1200 Pa, mammary tumor stiffness ranges from 2400 to 4800 Pa. To mimic the TME, we observed the behavior of clusters A and AC within the collagen gel (6 mg/mL) that has similar range of modulus to tumor stiffness at 0, 6, 12, 24, and 48 h.<sup>36,41</sup> Note that the 0 h time point indicates the time of injection of the clusters within the collagen gel. The live cell images (Figure 4a, Video S1(c), and Video S1(f)) and the fluorescence images (Figure 4b) display different behaviors of the cells in a time-dependent manner. Clusters A and AC showed similar behaviors until 6 h after embedding, after which the migration velocity of the cells rapidly increased after 12 h. The migration distance of both hASCs and MDA-MB-231 significantly increased in cluster AC ( $807.1 \pm 88 \mu\text{m}$ ), compared to that in cluster A ( $604.7 \pm 80 \mu\text{m}$ ) (Figure 4c).

Karnoub et al. found that CCL5 (chemokine ligand 5) enhances breast cancer cell migration, invasion, and metastasis from MSCs, which then acts in a paracrine effect on the cancer cells to induce their motility. Thus, MSCs accelerate the growth and invasion of breast cancer cells.<sup>42</sup> Moreover, MSCs and breast cancer cells via the formation of gap junctions favor the

exchange of exosomes and micro-RNAs that contribute to transforming MSC.<sup>43</sup> Furthermore, MSCs cocultured with breast cancer cells were reported to up-regulate EMT-associated genes.<sup>6</sup> Therefore, this may explain our observation where the cancer cells migrate farther distances when cocultured with hASCs.

**Migration and Invasion Markers in Cancer.** hASCs express markers including CD29, CD44, CD90, CD105, and CD166.<sup>24,44,45</sup> In particular, CD44 is a receptor that binds primarily to the extracellular glycosaminoglycan, hyaluronan. The engagement of CD44 by hyaluronan results in intracellular signaling that is linked to various effects such as cellular adhesion, migration, and invasion that are important in cancer progression.<sup>46–48</sup> In addition, purified cells from the stroma of human primary invasive breast carcinomas express a number of markers that are collectively used to characterize hMSCs. This implies that human carcinomas contain significant numbers of MSCs.<sup>42</sup> A recent report suggests CD44 plays a crucial role in the migration of MSC toward injured tissue.<sup>49</sup> Specially, CD44+/CD24– breast cancer cells exhibit increased invasive properties, which is an early progression necessary for metastasis.<sup>50</sup> According to our results, CD44 was expressed

by both clusters A and AC within the collagen gel at 48 h (Figure 5a,e). Particularly, cluster AC expressed a higher level of CD44 than cluster A. Comparable to a 2D culture, the hASCs and MDA-MB-231 suspension shows a high level of CD44 expression than that of hASCs or MDA-MB-231 alone (Figure S4). These results imply that cluster AC has more migration potential from a coculture environment, indicating that cluster AC can be utilized as an invasion model in breast tumor research.

ECM molecules, such as proteoglycans, fibronectin, collagen, laminin, hyaluronic acid, and other ECM components, play an important role in cell adhesion and migration.<sup>51,52</sup> As cancer cells undergo invasion and metastasis, they penetrate and attach to the matrix of target tissues.<sup>39</sup> In addition, MSC migration is regulated by fibronectin.<sup>53</sup> Likewise, we observed similar expression of fibronectin in migrated cells from outside the cluster (Figure 5b,e, not significant). We found that fibronectin was necessary for efficient migration of hASCs and MDA-MB-231 clusters A and AC toward the matrix.

Transforming growth factor beta-1 (TGF- $\beta$ 1) controls myofibroblast differentiation and promotes invasion of cancer cells.<sup>54</sup> In previous work, we discussed the expression of TGF- $\beta$ 1 from 3DCM formed hASCs such as cluster A.<sup>22</sup> We examined clusters A and AC using immunofluorescent staining of  $\alpha$ -SMA and confocal microscopy.  $\alpha$ -SMA expression was observed in the center of both clusters A and AC (Figure 5c,e). The result indicates that the putative myofibroblast of  $\alpha$ -SMA-positive cells are differentiated from the cells in the clusters.

Breast cancer cells are regulated by MSCs through cytokine networks such as IL6, IL8, CDCR4, CXCR7, and SDF-1 $\alpha$ .<sup>55–58</sup> Particularly, breast cancer cells express high levels of the CXCR4 receptor whose ligands are expressed on organs that represent important sites of breast cancer metastasis. CXCR4 is associated with organogenesis, hematopoiesis, and immune responses and can be located on ASCs. Figure 5d,e shows that the expression levels of CXCR4 from cluster A were comparable to those of cluster AC. They showed similar expression patterns of CXCR4 in clusters A and AC (not significant).

To investigate the migration and invasion of hASCs and breast cancer cells, we compared clusters A and AC within collagen gels at 48 h. We have already verified that a hypoxic cluster modulates its microenvironment to enhance angiogenic property by expression of cytokines.<sup>22–24</sup> Thus, our results demonstrate that clusters A and AC can regulate invasion by expression of cytokines such as CD44, fibronectin,  $\alpha$ -SMA, and CXCR4 from the cluster within the collagen gel. In addition, high density of collagen gel offered a similar environment to a solid TME, resulting in these cluster systems representing a biomimetic tissue of invading cancer cells.

## CONCLUSIONS

In conclusion, a novel method for mimicking 3D conditions for cancer migration and invasion was developed through the preparation of cell clusters within a collagen gel matrix. A methodology for mimicking 3D conditions has been pursued to prepare a spheroid-type 3D microtissue consisting stromal cell and cancer cell, cluster AC, by mixing hASCs and MDA-MB-231 on an artificial matrix. The migration activity such as morphological change, movements, and biochemical properties was higher in clusters AC than that in cluster A within a collagen gel matrix. In addition, fibronectin,  $\alpha$ -SMA, and CXCR4, typical markers, related to cell migration and invasion,

were expressed in cluster AC similar to in cluster A. Interestingly, CD44 expression was up-regulated in cluster AC compared to in cluster A, indicating that coexistence of the two cells increases CD44 expression. In this study we focus to establish and characterize a 3D tumor microenvironment to examine the effect of the interaction between stroma and cancer cells on cancer behaviors. A collagen-embedded 3D matrix of hASCs and cancer cells provides a platform for cancer research related to invasion and metastasis of cancer cells to aid in anticancer drug discovery.

## ASSOCIATED CONTENT

### Supporting Information

The Supporting Information is available free of charge on the ACS Publications website at DOI: 10.1021/acs.molpharmaceut.5b00953.

Cluster behavior within a collagen gel matrix (ZIP)  
Supporting Figures (PDF)

## AUTHOR INFORMATION

### Corresponding Authors

\*E-mail: skimbrc@kist.re.kr.

\*E-mail: kanwonlee@snu.ac.kr.

### Notes

The authors declare no competing financial interest.

## ACKNOWLEDGMENTS

This work was supported by the research resettlement fund for the new faculty of Seoul National University, SNU Invitation Program for Distinguished Scholar and a grant from the Korea Institute of Science and Technology (2E25497 & 2E25260).

## REFERENCES

- (1) Arguello, F.; Baggs, R. B.; Eskenazi, A. E.; Duerst, R. E.; Frantz, C. N. Vascular anatomy and organ-specific tumor growth as critical factors in the development of metastases and their distribution among organs. *Int. J. Cancer* **1991**, *48* (4), 583–590.
- (2) Gupta, G. P.; Massagué, J. Cancer Metastasis: Building a Framework. *Cell* **2006**, *127* (4), 679–695.
- (3) Fidler, I. J. Tumor Heterogeneity and the Biology of Cancer Invasion and Metastasis. *Cancer Res.* **1978**, *38* (9), 2651–2660.
- (4) Heppner, G. H. Tumor Heterogeneity. *Cancer Res.* **1984**, *44* (6), 2259–2265.
- (5) Reya, T.; Morrison, S. J.; Clarke, M. F.; Weissman, I. L. Stem cells, cancer, and cancer stem cells. *Nature* **2001**, *414* (6859), 105–111.
- (6) Martin, F. T.; Dwyer, R. M.; Kelly, J.; Khan, S.; Murphy, J. M.; Curran, C.; Miller, N.; Hennessy, E.; Dockery, P.; Barry, F. P.; O'Brien, T.; Kerin, M. J. Potential role of mesenchymal stem cells (MSCs) in the breast tumour microenvironment: stimulation of epithelial to mesenchymal transition (EMT). *Breast Cancer Res. Treat.* **2010**, *124* (2), 317–326.
- (7) Shimoyama, Y.; Nagafuchi, A.; Fujita, S.; Gotoh, M.; Takeichi, M.; Tsukita, S.; Hirohashi, S. Cadherin Dysfunction in a Human Cancer Cell Line: Possible Involvement of Loss of  $\alpha$ -Catenin Expression in Reduced Cell-Cell Adhesiveness. *Cancer Res.* **1992**, *52* (20), 5770–5774.
- (8) Friedrich, J.; Seidel, C.; Ebner, R.; Kunz-Schughart, L. A. Spheroid-based drug screen: considerations and practical approach. *Nat. Protoc.* **2009**, *4* (3), 309–324.
- (9) Chen, Y.-C.; Lou, X.; Zhang, Z.; Ingram, P.; Yoon, E. High-Throughput Cancer Cell Sphere Formation for Characterizing the Efficacy of Photo Dynamic Therapy in 3D Cell Cultures. *Sci. Rep.* **2015**, *5*, 12175.

- (10) Yamada, K. M.; Cukierman, E. Modeling Tissue Morphogenesis and Cancer in 3D. *Cell* **2007**, *130* (4), 601–610.
- (11) Kim, J. B. Three-dimensional tissue culture models in cancer biology. *Semin. Cancer Biol.* **2005**, *15* (5), 365–377.
- (12) Levental, K. R.; Yu, H.; Kass, L.; Lakins, J. N.; Egeblad, M.; Erler, J. T.; Fong, S. F. T.; Csiszar, K.; Giaccia, A.; Wenginger, W.; Yamauchi, M.; Gasser, D. L.; Weaver, V. M. Matrix Crosslinking Forces Tumor Progression by Enhancing Integrin Signaling. *Cell* **2009**, *139* (5), 891–906.
- (13) Wirtz, D.; Konstantopoulos, K.; Searson, P. C. The physics of cancer: the role of physical interactions and mechanical forces in metastasis. *Nat. Rev. Cancer* **2011**, *11* (7), 512–522.
- (14) Tracqui, P. Biophysical models of tumour growth. *Rep. Prog. Phys.* **2009**, *72* (5), 056701.
- (15) Dalton, B. A.; McFarland, C. D.; Underwood, P. A.; Steele, J. G. Role of the heparin binding domain of fibronectin in attachment and spreading of human bone-derived cells. *Journal of Cell Science* **1995**, *108* (5), 2083–2092.
- (16) Giancotti, F. G.; Ruoslahti, E. Integrin Signaling. *Science* **1999**, *285* (5430), 1028–1033.
- (17) Humphires, M. J.; Newham, P. The structure of cell-adhesion molecules. *Trends Cell Biol.* **1998**, *8* (2), 78–83.
- (18) Gallagher, J. T.; Turnbull, J. E. Heparan sulphate in the binding and activation of basic fibroblast growth factor. *Glycobiology* **1992**, *2* (6), 523–528.
- (19) Schlessinger, J.; Plotnikov, A. N.; Ibrahim, O. A.; Eliseenkova, A. V.; Yeh, B. K.; Yayon, A.; Linhardt, R. J.; Mohammadi, M. Crystal Structure of a Ternary FGF-FGFR-Heparin Complex Reveals a Dual Role for Heparin in FGFR Binding and Dimerization. *Mol. Cell* **2000**, *6* (3), 743–750.
- (20) Park, I.-S.; Han, M.; Rhie, J.-W.; Kim, S. H.; Jung, Y.; Kim, I. H.; Kim, S.-H. The correlation between human adipose-derived stem cells differentiation and cell adhesion mechanism. *Biomaterials* **2009**, *30* (36), 6835–6843.
- (21) Kang, J. M.; Han, M.; Park, I. S.; Jung, Y.; Kim, S. H.; Kim, S.-H. Adhesion and differentiation of adipose-derived stem cells on a substrate with immobilized fibroblast growth factor. *Acta Biomater.* **2012**, *8* (5), 1759–1767.
- (22) Park, I. S.; Rhie, J.-W.; Kim, S.-H. A novel three-dimensional adipose-derived stem cell cluster for vascular regeneration in ischemic tissue. *Cytotherapy* **2014**, *16* (4), 508–522.
- (23) Park, I. S.; Kim, S. H.; Jung, Y.; Rhie, J.-W.; Kim, S.-H. Endothelial Differentiation and Vasculogenesis Induced by Three-Dimensional Adipose-Derived Stem Cells. *Anat. Rec.* **2013**, *296* (1), 168–177.
- (24) Kim, J. H.; Park, I. S.; Park, Y.; Jung, Y.; Kim, S. H.; Kim, S.-H. Therapeutic angiogenesis of three-dimensionally cultured adipose-derived stem cells in rat infarcted hearts. *Cytotherapy* **2013**, *15* (5), 542–556.
- (25) Han, C.; Takayama, S.; Park, J. Formation and manipulation of cell spheroids using a density adjusted PEG/DEX aqueous two phase system. *Sci. Rep.* **2015**, *5*, 11891.
- (26) Wang, X.; Jung, Y.-S.; Jun, S.; Lee, S.; Wang, W.; Schneider, A.; Sun Oh, Y.; Lin, S. H.; Park, B.-J.; Chen, J.; Keyomarsi, K.; Park, J.-I. PAF-Wnt signaling-induced cell plasticity is required for maintenance of breast cancer cell stemness. *Nat. Commun.* **2016**, *7*, 10633.
- (27) Leung, B. M.; Leshner-Perez, S. C.; Matsuoka, T.; Moraes, C.; Takayama, S. Media additives to promote spheroid circularity and compactness in hanging drop platform. *Biomater. Sci.* **2015**, *3* (2), 336–344.
- (28) Benton, G.; DeGray, G.; Kleinman, H. K.; George, J.; Arnaoutova, I. *In Vitro* Microtumors Provide a Physiologically Predictive Tool for Breast Cancer Therapeutic Screening. *PLoS One* **2015**, *10* (4), e0123312.
- (29) Ivascu, A.; Kubbies, M. Rapid Generation of Single-Tumor Spheroids for High-Throughput Cell Function and Toxicity Analysis. *J. Biomol. Screening* **2006**, *11* (8), 922–932.
- (30) Montell, D. J. Morphogenetic Cell Movements: Diversity from Modular Mechanical Properties. *Science* **2008**, *322* (5907), 1502–1505.
- (31) Friedl, P.; Gilmour, D. Collective cell migration in morphogenesis, regeneration and cancer. *Nat. Rev. Mol. Cell Biol.* **2009**, *10* (7), 445–457.
- (32) Legant, W. R.; Pathak, A.; Yang, M. T.; Deshpande, V. S.; McMeeking, R. M.; Chen, C. S. Microfabricated tissue gauges to measure and manipulate forces from 3D microtissues. *Proc. Natl. Acad. Sci. U. S. A.* **2009**, *106* (25), 10097–10102.
- (33) Discher, D. E.; Janmey, P.; Wang, Y.-I. Tissue Cells Feel and Respond to the Stiffness of Their Substrate. *Science* **2005**, *310* (5751), 1139–1143.
- (34) Seewaldt, V. ECM stiffness paves the way for tumor cells. *Nat. Med.* **2014**, *20* (4), 332–333.
- (35) Wei, S. C.; Fattet, L.; Tsai, J. H.; Guo, Y.; Pai, V. H.; Majeski, H. E.; Chen, A. C.; Sah, R. L.; Taylor, S. S.; Engler, A. J.; Yang, J. Matrix stiffness drives epithelial-mesenchymal transition and tumour metastasis through a TWIST1-G3BP2 mechanotransduction pathway. *Nat. Cell Biol.* **2015**, *17* (5), 678–688.
- (36) Lam, C. R. I.; Wong, H. K.; Nai, S.; Chua, C. K.; Tan, N. S.; Tan, L. P. A 3D Biomimetic Model of Tissue Stiffness Interface for Cancer Drug Testing. *Mol. Pharmaceutics* **2014**, *11* (7), 2016–2021.
- (37) Kim, H.-D.; Peyton, S. R. Bio-inspired materials for parsing matrix physicochemical control of cell migration: A Review. *Integrative Biology* **2012**, *4* (1), 37–52.
- (38) Pan, Z.; Ghosh, K.; Hung, V.; Macri, L. K.; Einhorn, J.; Bhatnagar, D.; Simon, M.; Clark, R. A. F.; Rafailovich, M. H. Deformation Gradients Imprint the Direction and Speed of En Masse Fibroblast Migration for Fast Healing. *J. Invest. Dermatol.* **2013**, *133* (10), 2471–2479.
- (39) Hood, J. D.; Cheres, D. A. Role of integrins in cell invasion and migration. *Nat. Rev. Cancer* **2002**, *2* (2), 91–100.
- (40) Zaman, M. H.; Trapani, L. M.; Sieminski, A. L.; MacKellar, D.; Gong, H.; Kamm, R. D.; Wells, A.; Lauffenburger, D. A.; Matsudaira, P. Migration of tumor cells in 3D matrices is governed by matrix stiffness along with cell-matrix adhesion and proteolysis. *Proc. Natl. Acad. Sci. U. S. A.* **2006**, *103* (29), 10889–10894.
- (41) Tilghman, R. W.; Cowan, C. R.; Mih, J. D.; Koryakina, Y.; Gioeli, D.; Slack-Davis, J. K.; Blackman, B. R.; Tschumperlin, D. J.; Parsons, J. T. Matrix rigidity regulates cancer cell growth and cellular phenotype. *PLoS One* **2010**, *5* (9), e12905.
- (42) Karnoub, A.; Dash, A.; Vo, A.; Sullivan, A.; Brooks, M.; Bell, G.; Richardson, A.; Polyak, K.; Tubo, R.; Weinberg, R. Mesenchymal stem cells within tumour stroma promote breast cancer metastasis. *Nature* **2007**, *449*, 557–563.
- (43) Hass, R.; Otte, A. Mesenchymal stem cells as all-round supporters in a normal and neoplastic microenvironment. *Cell Commun. Signaling* **2012**, *10* (1), 26.
- (44) Yeon, B.; Park, M. H.; Moon, H. J.; Kim, S.-J.; Cheon, Y. W.; Jeong, B. 3D Culture of Adipose-Tissue-Derived Stem Cells Mainly Leads to Chondrogenesis in Poly(ethylene glycol)-Poly(L-alanine) Diblock Copolymer Thermogel. *Biomacromolecules* **2013**, *14* (9), 3256–3266.
- (45) Spaeth, E.; Klopp, A.; Dembinski, J.; Andreeff, M.; Marini, F. Inflammation and tumor microenvironments: defining the migratory itinerary of mesenchymal stem cells. *Gene Ther.* **2008**, *15* (10), 730–738.
- (46) Naor, D.; Sionov, R. V.; Ish-Shalom, D. CD44: Structure, Function and Association with the Malignant Process. In *Advances in Cancer Research*; George, F. V. W.; George, K., Eds.; Academic Press: 1997; Vol. 71, pp 241–319.
- (47) Droll, A.; Dougherty, S.; Chiu, R.; Dirks, J.; McBride, W.; Cooper, D.; Dougherty, G. Adhesive interactions between alternatively spliced CD44 isoforms. *J. Biol. Chem.* **1995**, *270* (19), 11567–11573.
- (48) Kosaki, R.; Watanabe, K.; Yamaguchi, Y. Overproduction of Hyaluronan by Expression of the Hyaluronan Synthase Has2 Enhances Anchorage-independent Growth and Tumorigenicity. *Cancer Res.* **1999**, *59* (5), 1141–1145.

(49) Herrera, M. B.; Bussolati, B.; Bruno, S.; Morando, L.; Mauriello-Romanazzi, G.; Sanavio, F.; Stamenkovic, I.; Biancone, L.; Camussi, G. Exogenous mesenchymal stem cells localize to the kidney by means of CD44 following acute tubular injury. *Kidney Int.* **2007**, *72* (4), 430–441.

(50) Sheridan, C.; Kishimoto, H.; Fuchs, R. K.; Mehrotra, S.; Bhat-Nakshatri, P.; Turner, C. H.; Goulet, R.; Badve, S.; Nakshatri, H. CD44(+)/CD24(-)breast cancer cells exhibit enhanced invasive properties: an early step necessary for metastasis. *Breast Cancer Research* **2006**, *8* (5), R59–R59.

(51) Ridley, A. J.; Schwartz, M. A.; Burridge, K.; Firtel, R. A.; Ginsberg, M. H.; Borisy, G.; Parsons, J. T.; Horwitz, A. R. Cell Migration: Integrating Signals from Front to Back. *Science* **2003**, *302* (5651), 1704–1709.

(52) Gumbiner, B. M. Cell Adhesion: The Molecular Basis of Tissue Architecture and Morphogenesis. *Cell* **1996**, *84* (3), 345–357.

(53) Veevers-Lowe, J.; Ball, S. G.; Shuttleworth, A.; Kielty, C. M. Mesenchymal stem cell migration is regulated by fibronectin through  $\alpha5\beta1$ -integrin-mediated activation of PDGFR- $\beta$  and potentiation of growth factor signals. *J. Cell Sci.* **2011**, *124* (8), 1288–1300.

(54) De Wever, O.; Mareel, M. Role of tissue stroma in cancer cell invasion. *Journal of Pathology* **2003**, *200* (4), 429–447.

(55) Zhang, X.; Xiao, D.; Wang, Z.; Zou, Y.; Huang, L.; Lin, W.; Deng, Q.; Pan, H.; Zhou, J.; Liang, C.; He, J. MicroRNA-26a/b Regulate DNA Replication Licensing, Tumorigenesis and Prognosis by Targeting CDC6 in Lung Cancer. *Mol. Cancer Res.* **2014**, *12*, 1535.

(56) Liu, S.; Ginestier, C.; Ou, S. J.; Clouthier, S. G.; Patel, S. H.; Monville, F.; Korkaya, H.; Heath, A.; Dutcher, J.; Kleer, C. G.; Jung, Y.; Dontu, G.; Taichman, R.; Wicha, M. S. Breast Cancer Stem Cells Are Regulated by Mesenchymal Stem Cells through Cytokine Networks. *Cancer Res.* **2011**, *71* (2), 614–624.

(57) Stuermer, E. K.; Lipenksy, A.; Thamm, O.; Neugebauer, E.; Schaefer, N.; Fuchs, P.; Bouillon, B.; Koenen, P. The role of SDF-1 in homing of human adipose-derived stem cells. *Wound Repair and Regeneration* **2015**, *23* (1), 82–89.

(58) Fernandis, A. Z.; Prasad, A.; Band, H.; Klosel, R.; Ganju, R. K. Regulation of CXCR4-mediated chemotaxis and chemoinvasion of breast cancer cells. *Oncogene* **2004**, *23* (1), 157–67.